Research Article

Received: 5 August 2016 Revised: 30 September 2016 Accepted article published: 5 October 2016 Published online in Wiley Online Library:

(wileyonlinelibrary.com) DOI 10.1002/jctb.5124

Removal of molybdate anions from contaminated waters by brown algae biomass in batch and continuous processes

Betina Carnevale,[a,b] Patricia Blanes,[a,b] Luis F Sala[a,b] and Sebastián E Bellú[a,b*]

Abstract

BACKGROUND: In recent years, the discharge of heavy metal ions in natural waters has become a serious problem. Among the various techniques that have been employed for heavy metal removal, adsorption is highly effective and economical because low-cost adsorbents can be employed. Brown algae are a potential biosorbent because of their high uptake capacities for various heavy metal ions. *Petalonia fascia* biomass immobilized in an agar matrix was tested as a new removal agent of Mo^{VI} from contaminated waters.

RESULTS: Sorption studies were performed in batch and continuous systems. *Petalonia fascia* has a high adsorption capacity (1376 ± 2 mg g^{-1}) at 20 °C and pH 1.0. Participation of hydroxyl and carboxylate functional groups in the adsorption of molybdate anions was confirmed by FT-IR analysis. SEM images showed that morphological surface changes happen after Mo^{VI} sorption. Mean free energies of sorption and activation parameters demonstrate that the sorption mechanism was chemical sorption. Mo^{VI} sorption onto brown seaweed surface was spontaneous and exothermic. *Petalonia fascia* has an energetically heterogeneous surface. Continuous sorption data were best fitted by a modified dose–response model. Scale-up of the sorption processes was achieved applying a bed depth service time (BDST) model. The critical bed depth, Z_0 was 1.7 cm.

CONCLUSIONS: *Petalonia fascia* biomass is a good adsorbent material for Mo^{VI} and it can be used in fixed bed columns for the purification of Mo^{VI} contaminated effluents. The high value of q_{max} and the low cost of this seaweed make this biomass a good sorbent for use in continuous treatment of groundwater and effluents contaminated with molybdate anions.

Supporting information may be found in the online version of this article.

Keywords: sorption; algae; decontamination; wastewater

INTRODUCTION

Marine algae are photosynthetic organisms that live in many environments on earth. They are abundant in the world's oceans and sea waters. Brown seaweed is usually a large macro-alga that has a high growth rate. Currently, brown alga biomass is being investigated to develop new applications in the field of water decontamination.[1]

In recent years, the discharge of heavy metal ions in natural waters has become a serious problem. Among the various techniques that have been employed for heavy metal removal, adsorption is highly effective and economical because low-cost adsorbents can be employed.[2] Algal biomasses have been employed in recent years to remove heavy metals cations such as Cu^{2+}, Zn^{2+} and Cd^{2+} [3–5], showing good performance to remediate effluents polluted with heavy metals cations. Toxic oxoanions such as CrO_4^{2-}, MoO_4^{2-} and ReO_4^- were also effectively removed from polluted effluents employing diverse algal biomasses.[6–8]

Brown algae are a potential biosorbent because of their high uptake capacities for various heavy metal ions due to the presence of biopolymers on the algae surface.

Molybdenum is a trace element that is present in plants and plays an important role in animal metabolism. It is harmful to plants at concentration higher than 5 µg g^{-1}, and for ruminants at concentrations higher than 10 µg g^{-1}.[9] Molybdenum has various industrial applications such as a constituent of electron tubes, high strength steel alloys and heat-resistant materials.[10] Pollution by molybdenum species in groundwater represents a great danger to populations where drinking water is obtained from wells. Mo^{VI} anions can cause water contamination if their concentration exceeds 5 mg L^{-1}.[11] As a consequence, the search for a

* *Correspondence to: S Bellú, Universidad Nacional de Rosario, Facultad de Ciencias Bioquímicas y Farmacéuticas, Suipacha 531, S2002LRK Rosario, Santa Fe, Argentina. Email: bellu@iquir-conicet.gov.ar; sbellu@fbioyf.unr.edu.ar*

a *Área Química General e Inorgánica, Departamento de Química-Física, Facultad de Ciencias Bioquímicas y Farmacéuticas, Universidad Nacional de Rosario, Suipacha 531, S2002LRK Rosario, Santa Fe, Argentina*

b *Instituto de Química de Rosario-CONICET, Suipacha 570, S2002LRK, Rosario, Santa Fe, Argentina*

groundwater/wastewater treatment process is very challenging. Simple sorption techniques have great advantages over traditional techniques,[12] as they are environmentally friendly, have low cost, mild operating conditions and high efficiency.

The aim of this study was the application of brown seaweed biomass as a new sorbent for Mo^{VI} sorption, in batch and continuous systems. In a previous work we reported the application of green seaweed in the removal of molybdate from contaminated waters.[13] Because brown seaweed is more abundant than green seaweed, and is low cost, it has been selected as a possible biomass source for molybdate removal from contaminated waters. The results obtained demonstrate the ability of brown seaweed to remove Mo^{VI} from water and support further implementation of the system to decontaminate water at greater scale.

MATERIALS AND METHODS

All chemicals were of analytical reagent grade and were used without further purification. Mo^{VI} solutions were obtained by dissolving specified amounts of $Na_2MoO_4.2H_2O$ in Milli-Q water.

Algal biosorbent

Petalonia fascia was collected at Puerto Madryn, Chubut, Argentina. *Petalonia fascia* biomass was washed with Milli-Q water, dried at 40 °C for 24 h, crushed and sieved ($0.3 <$ particle size < 0.5 mm). pH value at point of zero charge (pHpzc) was determined as described in the literature.[13]

Petalonia fascia fixed in agar

Petalonia fascia biomass ($0.3 <$ size < 0.5 mm) was mixed with 10.0 mL of agar solution (20.0 g L^{-1}) previously heated. The suspension was transferred to a Petri dish. Once the suspension solidified, it was cut into small squares, and stored at 8 °C in Milli-Q water.

Statistical experimental design

An experimental screening design was used to identify the key factors that significantly modified the response. A Plackett–Burman design was performed.[14] The factors studied were pH (pH = 1–10), sorbent dosage (m = 2–50 g L^{-1}), temperature (T = 20–60 °C) and contact time (t = 5–60 min), $[MoO_4^{2-}]_0 = 2.25$ mmol L^{-1}; batch volume = 10.0 mL.

After the screening design, an optimization design was performed. The optimized model was achieved employing Central Composite Design (CCD).[15] Once CCD was finished, a regression model was obtained for the response (mg Mo^{VI} sorbed g^{-1} brown algae). Analysis of variance (ANOVA) and other tests were applied to validate the model. Design Expert V. 7.0 software was used for mathematical calculations and statistical tests.

Batch sorption experiments

Petalonia fascia biomass was suspended in solutions containing different amounts of Mo^{VI}. The biomass dose was 2.0 ± 0.2 g L^{-1} at pH 1. Mo^{VI} concentration was determined spectrophotometrically at 400 nm.[16] Reproducibility of the analytical data was within 5%, estimated from triplicates analyses of the standard stock solutions.

The equipment was linearly calibrated from 0.8 mg L^{-1} to 50.0 mg L^{-1}. R^2 values of calibration curves were >0.995, and no trend was observed in the residuals for all samples analyzed. The calibration was checked after every 10 samples using homemade control solution and if the deviation was ±10%, the device was recalibrated. The quantification limit for this system was 0.05 mg L^{-1}. Replicate analyses of the batch sorption experiments were carried out to check the accuracy and precision of the result, which indicated variations within the range ± 5%.

Kinetic and thermodynamic studies were performed at three temperature values (20, 30 and 40 °C). Molybdate removal (q, mg g^{-1}) was calculated by the equation

$$q = \frac{(C_0 - C_t)\,V}{m} \tag{1}$$

where C_0 and C_t are the MoO_4^{2-} concentrations in solution (mg L^{-1}) at time 0 and t, respectively, V is the batch volume (L) and m is the quantity of sorbent used (g).

Continuous sorption experiments

The sorption of Mo^{VI} by *P. fascia* packed in glass columns 15 cm long and 1.4 cm internal diameter was studied. *Petalonia fascia* fixed in agar was packed under gravity into the columns keeping the package density constant. Upward flow of 0.50 mL min^{-1} was used. A solution containing 120 mg L^{-1} MoO_4^{2-} was pumped through the columns at pH 1.0 and room temperature. Samples of 1.0 mL were taken at different times and Mo^{VI} concentration was measured. The sorption capacity of molybdate ions was determined from the equation

$$q = \frac{C_0 Q}{1000\,m}\int_0^t \left(1 - \frac{C}{C_0}\right) dt \tag{2}$$

where q is the mass of metal sorbed (mg MoO_4^{2-} g^{-1} biomass); C_0 is the intake solution concentration (mg L^{-1}); C the outtake solution concentration (mg L^{-1}); m is the amount of biomass in the column (g) and Q is the volumetric flow (mL min^{-1}).

The column bed performance was described through a breakthrough curve, which was obtained by plotting C/C_0 against time. Breakthrough time (t_b, min) was defined for an effluent MoO_4^{2-} concentration of 5.0 mg L^{-1}. Saturation time (t_{sat}, min) was considered when $C/C_0 = 0.95$.

The Thomas model was applied to predict breakthrough curve behaviors. The expression for the Thomas model is given by the equation[17]

$$\frac{C}{C_0} = \frac{1}{1 + \exp\left(\frac{(q_{Th}m - C_0 vt)k_{Th}}{v}\right)} \tag{3}$$

where k_{Th} (L min^{-1} mg^{-1}) is Thomas rate constant, q_{Th} (mg g^{-1}) is the theoretical saturated sorption capacity, v (L min^{-1}) is the flow rate and m (g) is the sorbent mass.

A modified dose–response model was used,[18] described by the equation

$$\frac{C}{C_0} = 1 - \frac{1}{1 + \left(\frac{vt}{b}\right)^a} \tag{4}$$

where v (mL min^{-1}) is the flow rate. Parameters a and b are from the modified dose–response model.

FT-IR, SEM and EDAX analysis

FT-IR spectroscopy was performed using a Perkin Elmer FT-IR Spectrum One spectrophotometer in the range 400–4000 cm^{-1} employing KBr pellets. Surface structure of the brown algae was analyzed by scanning electron microscopy and Mo sorbed at the

surface was confirmed by EDAX microanalysis (SEM Fei model QUANTA 200 F, EDS EDAX with Si/Li detector). Experiments were done in Low Vacuum mode (LV 0.20–0.40 mbar chamber pressure), working distance (WD) 10–12 mm. Images were collected on non-coated samples at HV 10 kV, under low vacuum conditions. For semi-quantitative EDAX analysis of Mo, HV of 15 kV was employed. SEM and EDAX analysis were performed at LM CCT Rosario Laboratory.

RESULTS

FTIR analysis

The FT-IR spectra show numerous signals, indicating the complex composition of the brown seaweed (see Fig. 1).

Table 1 summarizes major stretching vibrations of *P. fascia* and *P. fascia*- Mo^{VI}.

After MoO_4^{2-} sorption by the alga, some changes in the FT-IR spectra arise. Stretching vibrations corresponding to Mo = O and Mo-O bonds appeared (1054 cm^{-1} and 616 cm^{-1}, respectively). The signal for Mo–O–Mo, suggest that polynuclear species of Mo^{VI} are present at the surface of *P. fascia*. The signal assigned to O–H stretching[19] was shifted and the C-O vibration was broadened. Antisymetric and symmetric stretching of –COO- were shifted. These changes suggest that both hydroxyl and carboxylate groups participate in binding of Mo^{VI} anions onto the surface of *P. fascia*.

Surface structures analysis

SEM images were collected for *P. fascia* surface analysis (see Fig. S1, Supplementary material). Figure S1 (A) and (B) show the surface structure of the brown alga. The brown seaweed surface presents cross-like structures in a random setup. After Mo^{VI} sorption, the surface displayed shrinkage of this structures (see Fig. S1 (C) and (D)). The results obtained are in concordance with those reported in literature,[13] in which modifications in surface morphology of green seaweed after Mo^{VI} removal was observed.

The brown algae cell wall is constituted predominantly of cellulose and its extracellular matrix is composed predominately of alginic acid.[20] Modifications in surface morphology were due to binding of the Mo^{VI} ions with biopolymers. This situation causes a contraction of the surface structures thus leading to shrinkage of the biopolymers present at the surface of *P. fascia*.

EDAX analysis of brown alga after molybdate removal performed at 20 kV voltage, displayed a signal corresponding to Mo at 2.4 keV (see Fig. S2), confirming that molybdenum was bonded to the surface of *P. fascia*.

Screening factorial design

Recognition of significant factors was made by Plackett Burman design (see Table S1, Supplementary Material). From the studied factors, sorbent dose and pH were significant ($P < 0.05$) and the last one has the major effect.

Optimization of the removal process

To enhance Mo^{VI} sorption removal, a central composite design strategy was employed to optimize the removal process (see Table S2). Experimental data were tested using multiple regression analysis. The equation that describes Mo^{VI} removal by *P. fascia* (q) was: The model was validated by analysis of variance (ANOVA) (see Table S3). The model F-value of 525.53 indicates the significance of the model. R^2 of the employed model was 0.9956, which is a high correlation value.

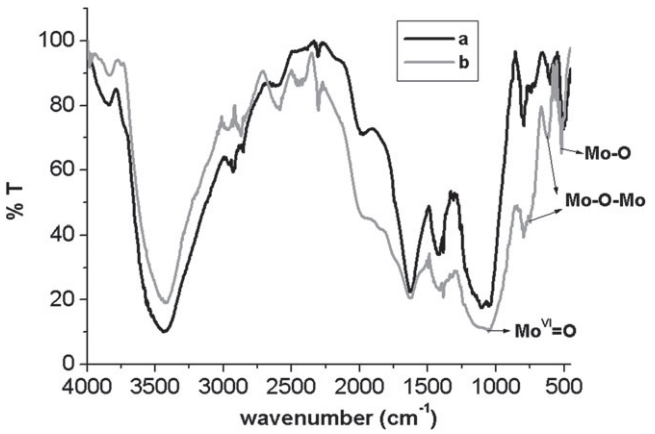

Figure 1. FTIR spectra of (a) native brown seaweed, (b) MoO_4^{2-} loaded brown seaweed.

$$q = 1.87 - 0.66\ \mathrm{pH} - 0.45\ m + 0.061\ \mathrm{pH}^2 \quad (5)$$

The 3D surface graph obtained by application of Equation (5), allowed the prediction of the molybdate removal at different pH and sorbent dose values (see Fig. S3).

The optimized model indicates that the highest removal of MoO_4^{2-} anions was achieved at pH 1.0 and sorbent dose 2.0 g L^{-1}. At this pH value, major Mo^{VI} species calculated by HYDRA and MEDUSA Programs[21] were $H_3Mo_7O_{24}^{3-}$ and H_2MoO_4 (see Fig. S4). The point of zero charge (pHpzc) of brown seaweed was 4.7(see Fig. S5). This means that at pH = 1, *P. fascia* surface is positively charged and attracts the heptamolybdate anions.

Optimal sorption conditions were corroborated experimentally. The experimental q value obtained (1.25 mg MoO_4^{2-} g^{-1} brown algae) was in agreement with the theoretical value obtained using Equation (5) (1.26 mg MoO_4^{2-} g^{-1} brown algae).

Sorption rate studies

Sorption rate studies allow the design of continuous bed sorption systems.[22] Pseudo-first and pseudo-second-order kinetic models were applied to describe sorption against time data.

The pseudo-first-order kinetic model is given by the equation

$$q_t = q_e\left(1 - e^{-k_1 t}\right) \quad (6)$$

where k_1 (min^{-1}) is the first-order-rate constant, q_e (mg g^{-1}) corresponds to the mass of molybdate in mg sorbed by 1 g of sorbent at equilibrium time, and q_t (mg g^{-1}) is the mass of molybdate in mg sorbed by 1 g of sorbent at time t.[23]

The pseudo-second-order kinetic model was expressed by the equation

$$q_t = \frac{t}{\left(\frac{1}{k_2 q_e^2} + \frac{t}{q_e}\right)} \quad (7)$$

where k_2 (min^{-1} g mg^{-1}) is the second-order-rate constant.[24]

Figure 2 shows the kinetic data and the best fit calculated by both models working at 20 °C.

As is seen in Fig. 2, the pseudo-second-order kinetic model offers the best prediction of the experimental results.

Most sorption processes occur through complex mechanisms.[13] The Weber and Morris diffusion model (Equation (8)[25] was applied to determine if intraparticle diffusion is a rate limiting step.

Table 1. Characteristic IR signal of *P. fascia* and *P. fascia*–Mo^{VI}

Sample	IR data (cm^{-1})						
	ν(O-H)	ν(C-O)	$\nu(C=O)_{antisym}$	$\nu(C=O)_{sym}$	ν(Mo-O)	ν(Mo=O)	ν(Mo-O-Mo)
P. fascia	3438	1100	1631	1425	-	-	-
P. fascia–Mo	3436	1100	1630	1420	616	1054	796

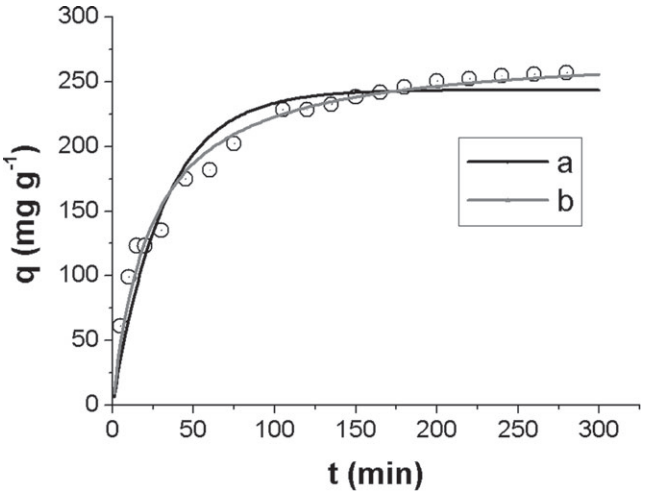

Figure 2. Kinetic data and best fit employing pseudo-first and second-order kinetic models. Biomass doses = 2.0 g L^{-1}; T = 20 °C; pH = 1.0; $[MoO_4^{2-}]_0$ = 0.0209 M; (a) first-order kinetic model; (b) second-order kinetic model.

Table 2. Characteristic parameters of the different kinetic models and coefficients of determination (R^2)

	T = 20 °C	T = 30 °C	TT = 40 °C
Pseudo-first-order			
q_e (mg g^{-1})	243 ± 5	185 ± 8	1 165 ± 4
k_1 (min^{-1})	0.032 ± 0.003	0.11 ± 0.02	0 0.15 ± 0.02
R^2	0.9285	0.8772	0 0.9258
Pseudo-second-order			
q_e (mg g^{-1})	275 ± 5	199 ± 6	176 ± 3
k_2 (min^{-1} g mg^{-1})	$1.53 \times 10^{-4} \pm 4 \times 10^{-6}$	$5.05 \times 10^{-4} \pm 8 \times 10^{-6}$	$1.29 \times 10^{-3} \pm 4 \times 10^{-5}$
R^2	0.9778	0.9701	0.9730
Intraparticle diffusion			
k_{id} (mg g^{-1} $min^{-0.5}$)	18.6 ± 0.7	18 ± 1	18 ± 2
R^2	0.6832	0.5808	0.0000

Biomass doses 2.0 g L^{-1}; pH = 1.0; $[MoO_4^{2-}]_0$ = 0.0209 mol L^{-1}

$$q_t = k_{id} t^{1/2} \quad (8)$$

where k_{id} (mg g^{-1} $min^{-1/2}$) is the intraparticle rate constant.

As can be seen from Fig. S6 inset, the removal process follows three distinct stages. Intraparticle diffusion and sorbate binding to active surface sites are rate limiting steps because the second segments of plots did not have zero intercept. This observation is in accordance with that reported in literature.[13] Table 2 gives the values of k_1, k_2, k_{id} and correlation coefficients obtained at three temperature values.

Table 3. Characteristic parameters of the different isotherm models and coefficients of determination (R^2)

	T 20 °C	T 30 °C	T 40 °C
Langmuir			
q_m (mg g^{-1})	1376 ± 2	1362 ± 2	1317 ± 1
K_L (L mg^{-1})	0.0170 ± 0.0006	0.0155 ± 0.0008	0.0139 ± 0.0002
R_L	0.540	0.563	0.590
R^2	0.9997	0.9997	0.9998
Freundlich			
K_F	39 ± 4	33 ± 4	26 ± 1
$1/n$	0.72 ± 0.03	0.75 ± 0.03	0.82 ± 0.01
R^2	0.9922	0.9936	0.9975
Sips			
q_m (mg g^{-1})	1040 ± 2	991 ± 1	981 ± 1
b	0.017 ± 0.001	0.016 ± 0.001	0.015 ± 0.001
N	1.18 ± 0.05	1.17 ± 0.05	1.04 ± 0.03
R^2	0.9993	0.9995	0.9995
D-R			
q_m (mg g^{-1})	880 ± 70	940 ± 90	1060 ± 30
β (mol^2 J^{-2}) × 10^9	6.7 ± 0.2	6.5 ± 0.2	6.48 ± 0.06
E (kJ mol^{-1})	8.64 ± 0.02	8.77 ± 0.03	8.78 ± 0.02
R^2	0.9962	0.9971	0.9992

Biomass doses 2.0 g L^{-1}; pH = 1.0; contact time: 6 h; $[MoO_4^{2-}]_0$ = 0.10–100.00 mg L^{-1}.

Table 4. Comparison between the sorption of Mo^{VI} by brown seaweed and by other sorbents reported in literature

Sorbent	Mo^{VI} uptake (mg g^{-1})	Reference
Organo-bentonite	224	30
Fe-biochar	78.5	31
La(III)-orange peel gel	195.2	32
Green seaweed	1280	13
Brown seaweed	1376	**This work**

Activation energy (E_a) of the removal process was calculated from the slope of the Arrhenius plot in its linealized form (see Fig. S7).

E_a value was 81.3 kJ mol^{-1}. E_a values for physical sorption are lower than 4.184 kJ mol^{-1}, on the other hand for chemisorptions, values of E_a higher than 8.4 kJ mol^{-1} are expected. The E_a value obtained in the present work supports a chemisorption mechanism.

Isotherm studies

Langmuir, Freundlich, Sips and Dubinin–Radushkevich isotherm models were applied to fit equilibrium experiments.

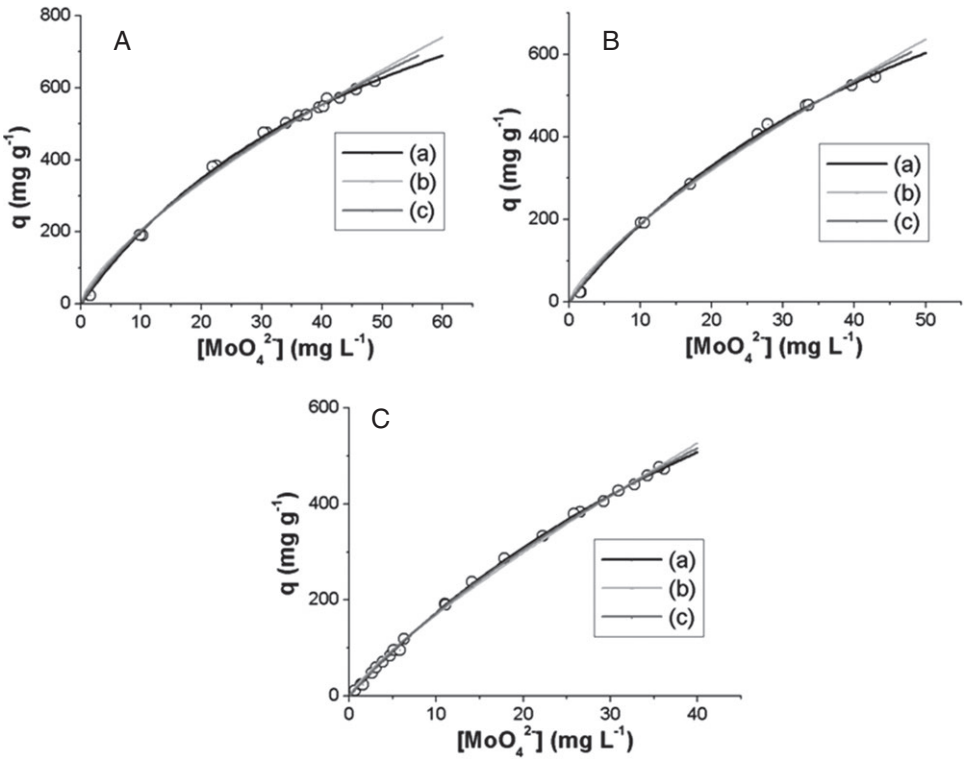

Figure 3. Sorption isotherm of molybdate ions onto brown seaweed. Biomass doses = 2.0 g L^{-1}; pH = 1.0; $[MoO_4^{2-}]_0$ = 0.10–100.00 mg L^{-1}; contact time 6 h. (A) 20 °C; (B) 30 °C; (C) 40 °C. (a) Langmuir model; (b) Freundlich model; (c) D-R model.

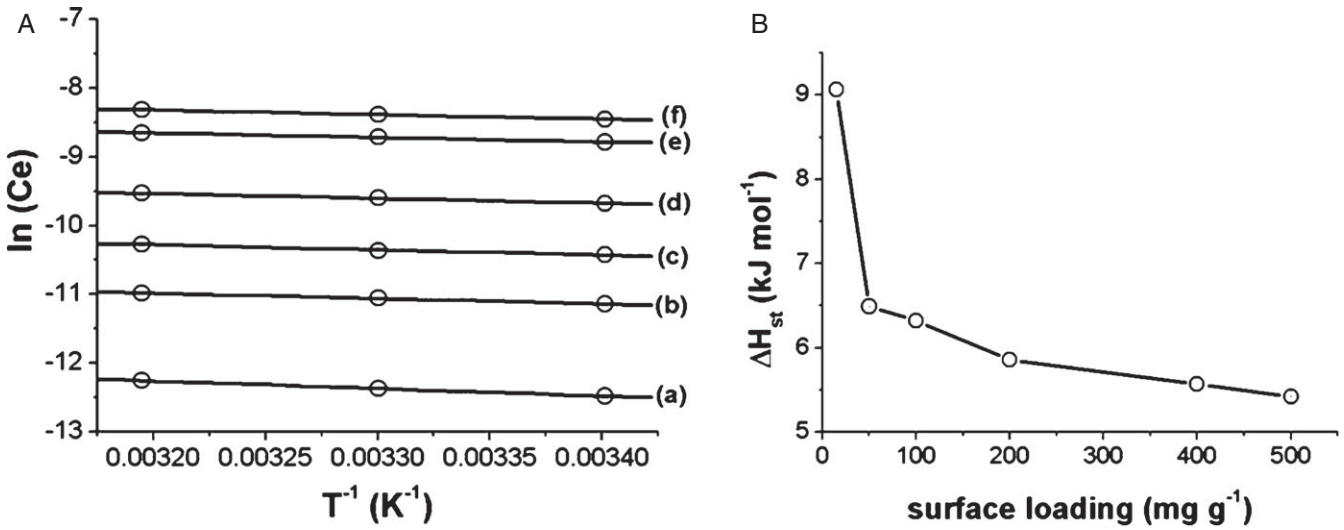

Figure 4. (A) Plots of ln Ce against T^{-1} for sorption of MoO_4^{2-} ions onto brown seaweed. (a) 15 mg g^{-1}; (b) 50 mg g^{-1}; (c) 100 mg g^{-1}; (d) 200 mg g^{-1}; (e) 400 mg g^{-1}; (f) 500 mg g^{-1}. (B) variation of isosteric heat of sorption with surface loading of MoO_4^{2-} ions onto brown seaweed.

The Langmuir isotherm model is expressed by the equation[26]

$$q_e = \frac{q_m K_L C_e}{1 + K_L C_e} \tag{9}$$

where C_e is the concentration of sorbate (mg L^{-1}) at equilibrium, q_m is the amount of sorbate required to form a monolayer (mg g^{-1}) and K_L is the Langmuir equilibrium constant.

The correct application of the Langmuir model can be inspected by applying the separation factor, R_L, expressed by the equation

$$R_L = \frac{1}{1 + K_L C_0} \tag{10}$$

where C_o is the highest Mo^{VI} anion concentration (mol L^{-1}). Sorption is favourable if $0 < R_L < 1$.

The Freundlich isotherm model is given by the equation[27]

$$q_e = K_F C_e^{1/n} \tag{11}$$

where K_F and $1/n$ are the Freundlich equilibrium constant and the coefficient of heterogeneity, respectively.

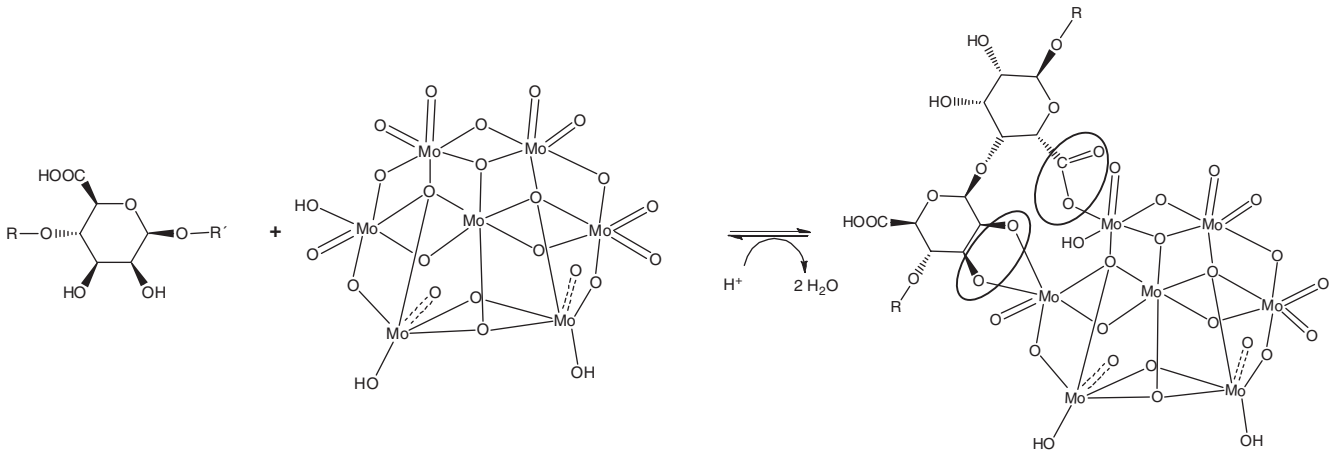

Scheme 1. Proposed mechanism for Mo^{VI} uptaking by brown seaweed.

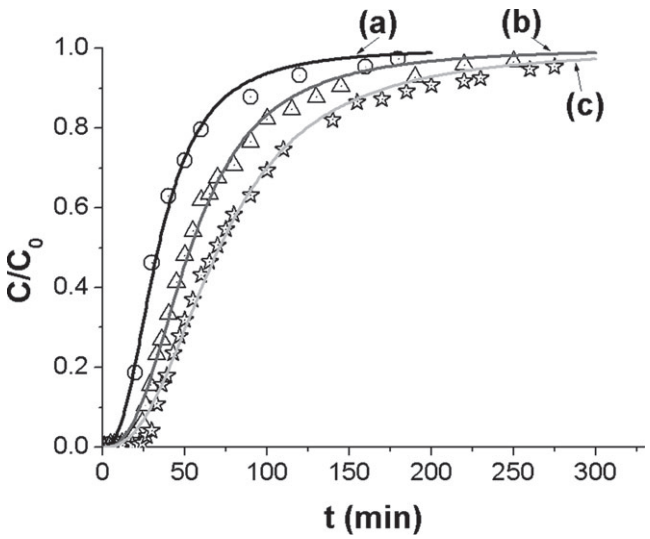

Figure 5. Breakthrough curves and modified dose–response models for different bed heights. $C_0 = 120$ mg L^{-1} MoO_4^{2-}; $Q = 0.50$ mL min^{-1}; $T = 20$ °C; pH = 1.0. (a) $h = 3.0$ cm; (b) $h = 4.5$ cm; (c) $h = 5.5$ cm.

The Sips isotherm model was applied in order to determine if the Langmuir or Freundlich model was the best isotherm model.[28] The Sips isotherm model is expressed by the equation

$$q_e = \frac{q_m b C_e^N}{1 + b C_e^N} \tag{12}$$

where q_m is the amount of sorbate required to form a monolayer (mg g^{-1}), b is the Sips constant and N is the Sips exponent.

The Dubinin–Radushkevich (D–R) isotherm model is given by the equation[29]

$$q_e = q_m e^{-\beta\varepsilon^2} \tag{13}$$

where β is a constant (mol^2 J^{-2}), ε is the Polanyi potential, which is equal to RT $\ln(1 + (1/C_e))$, and q_m the theoretical saturation capacity.

The constant β is related to the mean free energy E (kJ mol^{-1}) by the equation

$$E = \frac{1}{(2\beta)^{1/2}} \tag{14}$$

E values between 8 and 16 kJ mol^{-1}, show that the sorption mechanism is chemical sorption, since a physical mechanism always has values of E lower than 8 kJ mol^{-1}. The numerical values of E and other constants related to the isotherm models are tabulated in Table 3.

E values were in the range 8.6–8.8 kJ mol^{-1}, indicating that sorption occurs through a chemisorption mechanism. The maximum sorption capacity falls at higher T values, this result was previously reported in the literature,[13] and it was assigned to a partial degradation of the sorption sites with temperature. The R_L values show that the sorption process is favorable. Data obtained were well fitted by the Langmuir model at the three temperature values studied. Sips exponent (N) was quite close to unity at the three temperature values. This implies that use of the Langmuir isotherm model for this sorption system is appropriate.

Comparison of sorption capacity between *P. fascia* and other adsorbents is shown in Table 4.

The brown alga has a higher sorption capacity than other sorbents. Taking into account the cheapness of this seaweed, it is a better choice for use as an effective removal agent of molybdate anions.

Experimental data of Mo^{VI} sorption at various temperatures are shown in Fig. 3.

Thermodynamic studies

In industrial processes, values of thermodynamic parameters must be studied with the aim of determining the spontaneity of the process.

The sorption free energy change, $\Delta G°$, is defined by the equation[33]

$$\Delta G^\circ = -RT \ln 55.5\, K_L \tag{15}$$

where: K_L is the Langmuir constant (L mol^{-1}), and 55.5 is the water molarity (mol L^{-1}) .

For the determination of $\Delta H°$ and $\Delta S°$ the following equation was used:[33] The values of $\Delta H°$ and $\Delta S°$ obtained were −8.11 kJmol^{-1} and +71.55 j K^{-1} mol^{-1}, respectively. The positive value of $\Delta S°$ indicated an increase in randomness and the negative value of $\Delta H°$ confirmed the exothermic nature of the sorption process.

$$\ln 55.5 K_L = \frac{\Delta S^\circ}{R} - \frac{\Delta H^\circ}{R}\frac{1}{T} \tag{16}$$

Table 5. Different parameters for Thomas and modified dose–response models

	Thomas model				Modified dose–response model			
Z (cm)	$k_{Th} \times 10^4$	q_{Th}	R^2	χ^2	a	b	R^2	χ^2
3.0	7.8 ± 0.4	341 ± 5	0.9727	0.00504	2.5 ± 0.1	16.9 ± 0.3	0.9960	0.00074
4.5	4.7 ± 0.6	366 ± 6	0.9636	0.00498	2.6 ± 0.1	26.7 ± 0.4	0.9951	0.00067
5.5	3.6 ± 0.7	371 ± 2	0.9622	0.00506	2.5 ± 0.1	35.5 ± 0.2	0.9950	0.00067

$C_0 = 120$ mg L^{-1} MoO_4^{2-}
$Q = 0.50$ mL min^{-1}
T = 20 °C
pH = 1.0

Table 6. Different parameters for BDST model

C_t/C_0 %	$k_{BDST} \times 10^3$ (L mg^{-1} min^{-1})	N_0 (mg mL^{-1})	r^2
5	1.9 ± 0.6	291.8 ± 0.4	0.9994
20	1.7 ± 0.8	349.4 ± 0.5	0.9984
50	-	407.0 ± 0.4	0.9989
80	2.0 ± 0.7	798.8 ± 0.3	0.9997

$C_0 = 120$ mg L MoO_4^{2-}
$v = 0.32$ cm min^{-1}
T = 20 °C
pH = 1.0
$z = 3.0$; 4.5 and 5.5 cm.

Isosteric heat of sorption

Isosteric heat of sorption is a key thermodynamic parameter necessary to design removal processes[34]. This parameter can be calculated employing the Clausius–Clapeyron equation:[35] Plots of $\ln C_e$ versus T^{-1} were obtained at some q values and ΔH_{st} was calculated from the slope of these plots (Fig. 4(A)). The ΔH_{st} values are shown in Fig. 4(B) as a function of q values.

$$\frac{d \ln (C_e)}{dT} = -\frac{\Delta H_{st}}{RT^2} \tag{17}$$

Isosteric heat values fall with an increase in q, suggesting that the brown alga has an energetically heterogeneous surface. This behavior had previously been reported in the literature.[13]

Molybdate removal mechanism

Knowledge of the metal sorption mechanism allows improvement of the experimental conditions for metal removal by biomass. One of the possible sorption mechanisms is binding of toxic oxoanion to active surface groups present in the biomass[13].

Kinetic studies reveal that activation energy (E_a) is 81.3 kJ mol^{-1}. This value is in accordance with a chemisorption mechanism. Mean free energy of sorption (E) derived from the D-R model were in the range 8.6–8.8 kJ mol^{-1}. These E values also confirmed that the sorption mechanism is chemisorption.

Taking into account the results obtained in the present work we propose in Scheme 1, a chemisorption mechanism for molybdate removal by *P. fascia* surface biopolymers.

The presence of polynuclear heptamolybdate anions was postulated based on IR evidence. Carboxylate and hydroxyl functional groups were proposed as active binding sites, based on IR evidence. A similar chemisorption mechanism was reported in the literature, working with green seaweed as sorbent for Mo^{VI} ions.[13]

Fixed bed column studies

Breakthrough curves at three values of bed heights and a modified dose–response model best fit are plotted in Fig. 5.

Mo^{VI} ions uptake (mg g^{-1}), breakthrough and saturation time obtained experimentally are listed in Table S4. Table 5 shows the parameters of both mathematical models, and the correlation coefficients (R^2).

The values of q_{Th} were in agreement with the experimental q values. q_{Th} values were lower than the q_{max} obtained in batch experiments. These results indicate that in the continuous system, the availability of surface binding sites is lower than in a batch system.[36] The values of k_{Th} decrease as bed height increases, suggesting that the kinetic became slower at higher column heights This trend in k_{Th} with respect to column bed height was previously reported in the literature.[37]

Experimental data were better described by the modified dose–response model. R^2 values increased to 0.995–0.996, showing an excellent fit to the experimental data. The values of parameter b increased at high values of bed height. This trend was previously reported in the literature.[13]

Scale-up studies

Scale-up studies were performed applying the bed depth service time (BDST) model.[38]

Equation (18) expresses a linear function of the operation time with the bed depth:

$$t = \frac{N_0}{C_0 v} Z - \frac{1}{k_{BDST} C_0} \ln \left(\frac{C_0}{C} - 1 \right) \tag{18}$$

where N_0 is the sorption capacity (mg L^{-1}), v is the fluid velocity (cm min^{-1}) and k_{BDST} is the kinetic constant (L mg^{-1} min^{-1}).

Iso-concentration lines for Mo^{VI} anions sorption in a fixed bed at four C/C_0 ratios were calculated (see Fig. S8).

Table 6 shows the k_{BDST} and N_0 parameters obtained for different C/C_0 ratios.

N_o values at low breakthrough condition were lower than the full bed capacity of the biomass because on the *P. fascia* surface, some active sites remain free at lower C_t/C_0 value.[38] The rate constant, k_{BDST}, remains the same in the C_t/C_0 range employed.

The BDST model was validated by inspection of the breakthrough curve at 50%. In this condition, $C_0/C = 2$, therefore, the logarithmic term of the BDST equation is equal to zero. Good fitting was achieved at 50% breakthrough validating application of the BDST model to the sorption process of Mo^{VI} by

P. fascia biomass. The critical bed depth, Z_0 is obtained by the equation

$$Z_0 = \frac{v}{k_{BDST} N_0} \ln\left(\frac{C_0}{C_b} - 1\right) \quad (19)$$

The critical bed depth, Z_0 was equals to 1.7 cm. This value corresponds to the minimum theoretical bed height of *P. fascia* biomass that produces an effluent concentration at $t = 0$ lower than the breakthrough concentration.

CONCLUSIONS

We report the application of brown seaweed, as a new sorbent of Mo^{VI} ions. Participation of hydroxyl and carboxylic groups in the binding of Mo^{VI} anions at the surface of *P. fascia* was confirmed by FT-IR analysis. Kinetic and thermodynamic parameters confirm that the removal mechanism was chemical sorption. Continuous sorption data were analyzed applying three models. The high value of q_{max} and the low cost of this seaweed make this biomass a good sorbent for use in continuous treatment of groundwater and effluents contaminated with molybdate anions.

ACKNOWLEDGEMENTS

We thank the National Research Council of Argentina (CONICET) PIP 0037, National Agency of Scientific and Technological Promotion (ANPCyT) PICT 2014–0529 and National University of Rosario (UNR) BIO344 for financial support. We also thank the Argentine Technological Founding of Environmental and Social Development, for equipment donation.

Supporting Information

Supporting information may be found in the online version of this article.

REFERENCES

1 Song M, Pham HD, Seon J and Woo HC, Marine brown algae: a conundrum answer for sustainable biofuels production. *Renew Sustain Energy Rev* **50**:782 – 792 (2015).
2 Kwak HW, Kim MK, Lee JY, Yun H, Kim MH, Park YH *et al.*, Preparation of bead-type biosorbent from water-soluble *Spirulina platensis* extracts for chromium (VI) removal. *Algal Res* **7**:92–99 (2015).
3 Rajfur M, Kłos A and Wacławek M, Sorption properties of algae *Spirogyra* sp. and their use for determination of heavy metal ions concentrations in surface water. *Bioelectrochemistry* **80**:81–86 (2010).
4 Rajfur M, Kłos A and Wacławek M, Sorption of copper(II) ions in the biomass of alga *Spirogyra* sp. *Bioelectrochemistry* **87**:65–70 (2012).
5 Kłos A and Rajfur M, Influence of hydrogen cations on kinetics and equilibria of heavy-metal sorption by algae – sorption of copper cations by the alga *Palmaria palmata* (Linnaeus) Weber and Mohr (Rhodophyta). *J Appl Phycol* **25**:1387–1394 (2013).
6 Javadian H, Ahmadi M, Ghiasvand M, Kahriz S and Katal R, Removal of Cr(VI) by modified brown algae *Sargassum bevanom* from aqueous solution and industrial wastewater. *Taiwan Inst Chem Eng* **44**:977–989 (2013).
7 Jayakumar R, Rajasimman M and Karthikeyan C, Sorption of hexavalent chromium from aqueous solution using marine green algae *Halimeda gracilis*: optimization, equilibrium, kinetic, thermodynamic and desorption studies. *J Chem Eng* **2**:1261–1274 (2014).
8 Lou Z, Wang J, Jin X, Wan L, Wang Y, Chen H *et al.*, Brown algae based new sorption material for fractional recovery of molybdenum and rhenium from wastewater. *Chem Eng J* **273**:231–239 (2015).
9 Goldberg S, Lesch SM and Suarez DL, Predicting molybdenum adsorption by soils using soil chemical parameters in the constant capacitance model. *Soil Sci Soc Am J* **66**:1836–1842 (2002).
10 Bei H, Shim S, George E, Miller M, Herbert E and Pharr G, Compressive strengths of molybdenum alloy micropillars prepared using a new technique. *Scr Mater* **57**:397–400 (2007).
11 Moret A and Rubio J, Sulphate and molybdate ions uptake by chitin-based shrimp shells. *J Mineral Eng* **16**:715–722 (2003).
12 Vijayaraghavan K and Balasubramanian R, Is biosorption suitable for decontamination of metal-bearing wastewaters? *A critical review on the state-of-the-art of biosorption processes and future directions. J Environ Manage* **160**:283–296 (2015).
13 Bertoni FA, Medeot AC, Gonzalez JC, Sala LF and Bellu SE, Application of green seaweed biomass for Mo^{VI} sorption from contaminated waters. Kinetic, thermodynamic and continuous sorption studies. *J Colloid Interf Sci* **446**:122–132 (2015).
14 Bruns RE, Scarmino IS and de Barros Neto B, *Statistical Design - Chemometrics*, 1st edn. Elsevier, Amsterdam (2006).
15 Bezerra MA, Santelli REE, Oliveira P, Villar LS and Esclaleira LA, Response surface methodology (RSM) as a tool for optimization in analytical chemistry. *Talanta* **76**:965–977 (2008).
16 Soni R and Bartusek M, Molybdate complexes with *o*-diphenols. *J Inorg Nuclear Chem* **33**:2557–2563 (1971).
17 Thomas HC, Heterogeneous ion exchange in a flowing system. *J Am Chem Soc* **66**:1664–1666 (1944).
18 Yan G, Viraraghavan T and Chen M, A new model for heavy metal removal in a biosorption column. *Adsorp Sci Technol* **19**:25–43 (2001).
19 Pérez Marín AB, Aguilar MI, Meseguer VF, Ortuño MF, Sáez J and Lloréns M, Biosorption of chromium (III) by orange (*Citrus cinensis*) waste: batch and continuous studies. *Chem Eng J* **155**:199–206 (2009).
20 Murphy V, Tofail S, Hughes H and McLoughlin P, A novel study of hexavalent chromium detoxification by selected seaweed species using SEM-EDX and XPS analysis. *Chem Eng J* **148**:425–433 (2009).
21 Medusa Program (http://www.kemi.kth.se/medusa).
22 Hawari A, Rawajfih Z and Nsour N, Equilibrium and thermodynamic analysis of zinc ions adsorption by olive oil mill solid residues. *J Hazard Mater* **168**:1284–1289 (2009).
23 Lagergren S, About the theory of so-called adsorption of soluble substances. *Handlingar* **24**:1–39 (1898).
24 Ho YS and McKay G, About the theory of so-called adsorption of soluble substances. *Process Biochem* **34**:451–465 (1999).
25 Weber WJ and Morris JC, Kinetics of adsorption on carbon from solution. *J Sanit Eng Div ASCE* **89**:31–59 (1963).
26 Langmuir I, The adsorption of gases on plane surfaces of glass, mica and platinum. *J Am Chem Soc* **40**:1361–1403 (1918).
27 Freundlich HMF, Uber die adsorption in losungen. *Z Phys Chem* **57**:385– 470 (1906).
28 Sips R, On the structure of a catalyst surface. *J Chem Phys* **16**:490–495 (1948).
29 Dubinin MM and Radushkevich LV, Equation of the characteristic curve of activated charcoal. *Proc Acad Sci USSR Phys Chem Sect* **55**:331–333 (1947).
30 Dodbiba G, Fujit T, Kikuchi T, Manjanna J, Matsuo S, Takahashi H *et al.*, Synthesis of iron-based adsorbents and their application in the adsorption of molybdenum ions in nitric acid solution. *Chem Eng J* **166**:496–503 (2011).
31 Johansson CL, Paul NA, de Nys R and Roberts DA, Simultaneous biosorption of selenium, arsenic and molybdenum with modified algal-based biochars. *J Environ Manage* **165**:117–123 (2016).
32 Shan W, Fang D, Zhao Z, Shuang Y, Ning L, Xing Z *et al.*, Application of orange peel for adsorption separation of molybdenum(VI) from Re-containing industrial effluent. *Biomass Bioenergy* **37**:289–297 (2012).
33 Chen S, Yue Q, Gao B, Li Q and Xu X, Removal of Cr(VI) from aqueous solution using modified corn stalks: characteristic, equilibrium, kinetic and thermodynamic study. *Chem Eng J* **168**:909–917 (2011).
34 Sircar S, Heat of adsorption on heterogeneous adsorbents. *Appl Surf Sci* **252**:647–653 (2005).
35 Unnithan MR and Anirudhan TS, The kinetics and thermodynamics of sorption of chromium(VI) onto the iron(III) complex of a carboxylated polyacrylamide-grafted sawdust. *Ind Eng Chem Res* **40**:2693–2701 (2001).
36 Bulgariu D and Bulgariu L, Sorption of Pb(II) onto a mixture of algae waste biomass and anion exchanger resin in a packed-bed column. *Bioresource Technol* **129**:374–380 (2013).
37 Song J, Zou W, Bian Y, Su F and Han R, Adsorption characteristics of methylene blue by peanut husk in batch and column modes. *Desalination* **265**:119–125 (2011).
38 Bohart GS and Adams EQ, Behavior of charcoal towards chlorine. *J Chem Soc* **42**:523–529 (1920).

